Energy & Environmental Science

Levelized cost and carbon intensity of solar hydrogen production from water electrolysis using a scalable and intrinsically safe photocatalytic Z-scheme electrochemical raceway system

Journal:	*Energy & Environmental Science*
Manuscript ID	EE-ART-12-2024-005889.R1
Article Type:	Paper
Date Submitted by the Author:	26-Apr-2025
Complete List of Authors:	Collins, Stephanie; Lawrence Berkeley National Laboratory, Energy Analysis and Environmental Impacts Division, Energy Technology Area Acevedo, Yaset; Strategic Analysis Inc Esposito, Daniel; Columbia University, Chemical Engineering Bala Chandran, Rohini; University of Michigan, Mechanical Engineering Ardo, Shane; University of California, Chemistry James, Brian; Strategic Analysis Inc Breunig, Hanna; Lawrence Berkeley National Laboratory, Energy Analysis and Environmental Impacts Division, Energy Technology Area

Broader Context Statement:

Levelized cost and carbon intensity of solar hydrogen production from water electrolysis using a scalable and intrinsically safe photocatalytic Z-scheme electrochemical raceway system

Stephanie Collins*[a], Yaset Acevedo[*b], Daniel V. Esposito[c], Rohini Bala Chandran[d], Shane Ardo[e], Brian D. James[*†b], Hanna Breunig[*†a]

a. Energy Analysis and Environmental Impacts Division, Energy Technology Area, Lawrence Berkeley National Laboratory, Berkeley, California, U.S.A., 94720
b. Strategic Analysis Inc., Arlington, Virginia, U.S.A., 22203
c. Columbia University, New York, New York, U.S.A., 10027
d. University of Michigan, Ann Arbor, Michigan, U.S.A., 48109
e. University of California, Irvine, Irvine, California, U.S.A., 92697
* These authors contributed equally to this work.
† Co-corresponding authors

Hydrogen generation from renewable resources represents a critical pathway to a low-carbon energy future, with significant potential to mitigate greenhouse gas emissions in sectors like industry and transportation. Traditional approaches to hydrogen production rely on hydrocarbon feedstocks or using electricity to power electrolysis, which raises around emissions accounting. Photoelectrochemical hydrogen production offers an innovative alternative, directly harnessing solar energy to split water into hydrogen and oxygen, bypassing the need for intermediate electricity generation. Despite its promise, existing designs for photoelectrochemical systems have faced economic challenges, with costs remaining uncompetitive compared to scaled conventional electrolysis. In this context, a novel Type 2 "Z-scheme" photocatalytic reactor design emerges as a potential low-cost and low-carbon solution, utilizing advanced suspended semiconducting nanoconductors in a raceway configuration to achieve efficient solar-to-hydrogen conversion. In this work, we demonstrate both cost and carbon intensity advantages of this raceway concept, positioning it as a scalable and sustainable hydrogen production technology. These findings underscore the need for further experimental validation and prototyping, paving the way for next-generation renewable hydrogen solutions.

ARTICLE

Levelized cost and carbon intensity of solar hydrogen production from water electrolysis using a scalable and intrinsically safe photocatalytic Z-scheme electrochemical raceway system

Received 00th January 20xx,
Accepted 00th January 20xx

DOI: 10.1039/x0xx00000x

Stephanie Collins*[a], Yaset Acevedo*[b], Daniel V. Esposito[c], Rohini Bala Chandran[d], Shane Ardo[e], Brian D. James[†b], Hanna Breunig[†a]

Generating hydrogen from renewable resources would unlock a low-carbon energy carrier that could be used to reduce greenhouse gas emissions in sectors such as industry and transportation. Yet, the allocation of new or existing renewable electricity generation solely to hydrogen production remains contentious due to disputes regarding emissions accounting. Photocatalytic (PC) hydrogen production technologies offer a unique solution, as hydrogen is produced directly from solar energy and water, without the need for electricity generation. However, cost projections for all photocatalytic designs to date have suggested that they are not cost competitive compared to conventional electrolysis systems manufactured at scale. Herein, we offer the first illustrative benchmark of cost and carbon intensity of hydrogen produced in a Type 2 "Z-scheme" photocatalytic reactor design, which employs suspended semiconducting nanoconductor particles organized into two stacked volumes in a raceway design. The "Z-scheme" system utilizes two separate photoabsorber particles, tuned to drive either the hydrogen evolution reaction or the oxygen evolution reaction individually, connected via a reversible, charge transfer redox couple in solution. The results suggest a highly competitive and scalable technology, that justifies further experimental validation and prototyping in the field.

Introduction

The realization of an environmentally sustainable and widely-adopted hydrogen economy may require lowering hydrogen production costs of pathways with ultra-low greenhouse gas emissions to \$1 kg^{-1} H_2.[1] Hydrogen at 20 bar produced from steam methane reforming has a carbon intensity (CI) of 9-10 kg CO_2 equivalents (CO_2eq) per kg H_2. Meeting carbon intensity targets such as the 4 kg CO_2eq per kg H_2 used to define "clean hydrogen" in the United States Inflation Reduction Act, or the 2 kg CO_2eq per kg H_2 set by the Infrastructure Investment and Jobs Act, requires a low-carbon power source, as roughly 90% of the carbon intensity of hydrogen from water electrolysis is attributed to the source of electricity. While water splitting technologies have the advantage of zero direct carbon emission, the extent to which the cost of liquid alkaline or proton exchange membrane (PEM) electrolysis can be reduced may be limited, as these technologies rely on rare metals such as platinum and iridium and must be coupled with an external power source, such as a photovoltaic system or grid connection. Without even considering hydrogen distribution and storage costs, pathways for water splitting such as commercial liquid alkaline and PEM electrolysis systems can generate H_2 at \$5 to \$6 kg^{-1}, with projected potential cost savings in manufacturing and upscaling lowering costs to \$2 kg^{-1}.[2] These costs assume high capacity factors (number of hours of operation) due to being grid-tied, whereas fully renewable photovoltaic powered electrolysis will be more expensive (\$5-7 kg^{-1}).[3,4] When using nuclear, solar, or wind, carbon intensities below 1 kg CO_2eq per kg H_2 can be achieved, compared with using natural gas powered grid electricity where the carbon intensity can be as high as 17 kg CO_2eq per kg H_2.[5]

In an effort to further lower costs, alternative H_2 production pathways are being explored, including integrated solar fuel generators such as integrated photoelectrochemical (PEC) devices,[6] photocatalytic sheets,[7] and photocatalytic suspension reactors.[8,9] In contrast to a more conventional coupled photovoltaic-electrolysis system, these emerging pathways conduct the light harvesting and water splitting steps simultaneously within an integrated, all-in-one device or reactor that presents opportunities to reduce capital costs and/or increase solar-to-hydrogen (STH) conversion efficiency. STH efficiency is defined as the amount of chemical energy (lower heating value) contained in the H_2 produced divided by the solar energy input, after correction for additional external bias.[10] Many proposed systems are designed with PEC electrodes requiring multiple semiconductor, catalytic, and/or protective layers comprised of different materials to achieve

[a] Energy Analysis and Environmental Impacts Division, Energy Technology Area, Lawrence Berkeley National Laboratory, Berkeley, California, U.S.A., 94720
[b] Strategic Analysis Inc., Arlington, Virginia, U.S.A., 22203
[c] Columbia University, New York, New York, U.S.A., 10027
[d] University of Michigan, Ann Arbor, Michigan, U.S.A., 48109
[e] University of California, Irvine, Irvine, California, U.S.A., 92697
* These authors contributed equally to this work.
† Co-corresponding authors
Electronic Supplementary Information (ESI) available: [details of any supplementary information available should be included here]. See DOI: 10.1039/x0xx00000x

targeted performance metrics such as durability and STH efficiency.[7] A wealth of research has emerged around the development of photocatalytic nano-to-micron sized particle agglomerates that can be used to absorb sunlight and drive water splitting when illuminated.[11]

Several studies have sought to benchmark the potential cost and energy intensity of these emerging solar fuel systems.[6,12–14] For example, the findings of Pinaud et al. suggest that particle suspension reactor designs can lead to low hydrogen production costs of \$2 to \$4 kg^{-1}.[6] Particle suspension reactor designs have been proposed and are referred to as Type 1 and Type 2. Type 1 reactor designs have a simpler layout, where the hydrogen evolution reaction (HER) and the oxygen evolution reaction (OER) occur in the same compartment, raising safety and gas separation concerns. Type 2 requires a Z-scheme reactor design in which hydrogen and oxygen evolve in separate compartments, connected via a soluble or solid-state mediator between the two photoabsorbers. Type 2 reactor designs address the safety and gas separation concern, but potentially introduce losses associated with the transport of ions between beds and generally kinetically facile undesirable back reactions.

In addition to evaluating the cost of such emerging designs, the environmental impact and greenhouse gas emissions must also be considered. Life-cycle assessment (LCA) is a method used to quantitatively evaluate the environmental impacts of processes and technologies. Numerous LCAs of hydrogen production via electrolysis have been published,[15–17] with results ranging from resource and water consumption to energy and greenhouse gas emission intensities. However, the authors are aware of only one LCA of PC, and only of a Type 3 PC stacked cell design, which are fixed array panels.[18] Results of this LCA are not transferrable to suspended particle configurations, making it difficult to evaluate the carbon intensity of the most promising emerging designs for PC.

In this study, we address this gap by conducting a coupled technoeconomic analysis (TEA) and LCA of a photocatalytic Type 2 facility that employs suspensions of photocatalytic nanoparticles in a raceway configuration (**Figure 1**). We develop the first conceptual design and associated material and energy balances for prototypical nanoparticles and raceway designs that are suitable for the HER/OER reactions. Compared to previous embodiments of Type 2 photocatalytic reactor designs (such as those in Pinaud et al.), the raceway design uses large bulk sheet materials which simplify manufacturing and deployment, and increase economies of scale.[6] This leads to a lower \$/m^2 of deployed reactor area, increasing the economic feasibility of this design. The total installed capital cost, production cost (i.e. levelized cost of hydrogen: LCOH), and environmental impacts of produced hydrogen are calculated for two raceway facility concepts: a small, 1,000 kg H_2/day scale facility (roughly equivalent to a 2.4 MW liquid alkaline electrolyzer) and a large, 50,000 kg H_2/day scale facility (roughly equivalent to a 116 MW liquid alkaline electrolyzer). We show that low-cost designs can achieve carbon intensities at or lower than solar-powered water electrolysis systems. Furthermore, the facilities have a low land footprint (1,050 acre for 50 MTD plant), water footprint (3.78 gal/kg H_2), and provide

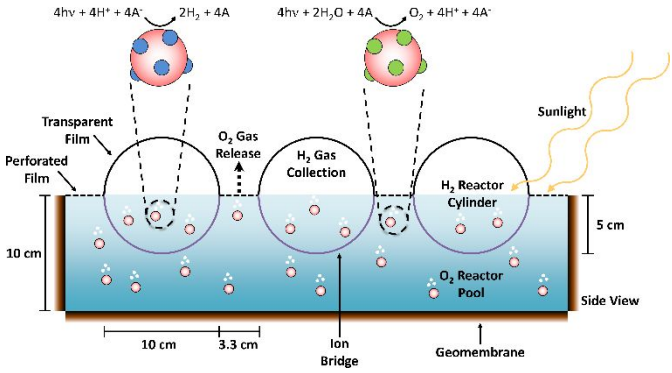

Figure 1. Schematic of photocatalytic Type 2 Z-Scheme raceway design with hydrogen reactor cylinders floating on an oxygen reactor raceway pool. Suggested dimensions used to estimate raceway costs although additional tuning will be needed to accommodate passive diffusion and natural convection of the solution.

opportunities for full-time job creation (63 jobs for 50 MTD plant). We explore how changes in electric power sources and key technical targets such as STH efficiency and materials lifespan impact the overall carbon intensity. This work is illustrative of a potential future system with as-yet unattained levels of STH and durability, and models baseline nanoparticles using Fe_2O_3 and TiO_2 as placeholders for materials in development. The raw materials cost and LCA are based on Fe_2O_3 and TiO_2 as example photocatalyst materials that have been extensively studied by the field, while the modelled STH efficiencies are assumed to be achieved by yet-to-be developed composite photocatalyst particles that are comprised of an earth-abundant photoabsorber material with similar sourcing, manufacturing, and carbon footprint as Fe_2O_3 and TiO_2. State-of-the-art metal oxide materials including pure and doped WO_3, $SrTiO_3$, and $BiVO_4$ can be readily substituted into the cost analysis once they have achieved desired performance targets.[19–21]

As highlighted in **Figure S6**, opportunities for lowering the carbon intensity of this design are limited, but relatively straightforward, and include using low-carbon electricity for ancillary equipment and reducing plastic consumption. This could be achieved by designing reactor volumes to be highly durable to outdoor conditions and operational wear, or through advanced reactors that could rely on a solid or soluble mediator rather than plastic reactors.[6] The principle research challenge will be with respect to demonstrating a nanoparticle catalyst that can achieve an STH efficiency of ≥10%, which will be required to achieve <\$2 kg^{-1} H_2 with the current raceway plant concept. This is already underway, and we hope with the results reported herein that such efforts will be amplified in both interest and financial support, because this pathway may then be viable, and the lowest-cost option in this space. New designs have emerged that allow reactor beds to be stacked vertically rather than positioned side by side, such as the one evaluated in Pinaud, et al.[6] Adjacent volumes that separate H_2 and O_2 evolution reactions can have challenges with respect to mediator transport fluxes across the ion bridges, as well as the low maximum STH efficiency achievable (<15.5%).[6] Additionally, focus on larger scale production plants will help to lower the

electricity emissions associated with compression and purification.

The assessment of environmental impacts beyond carbon intensity can be found in **Table S8** and **Figure S7** where freshwater ecotoxicity (defined as toxicity towards species living in freshwater environments) shows a substantial impact by way of material consumption similar to CI. Plastics, platinum, and steel production processes lead to significant impacts along with electricity generation. These material contributions primarily hold true for all other impact categories assessed in this study; however their relative magnitudes are negligible in comparison to ecotoxicity, and CI which is the primary focus of this study.

Methodology

System definition

For comparison with previous PC studies, the plant site is assumed to be Daggett, CA, USA, at 35° North latitude, due to having a good solar resource and limited cloud cover.[6] Bed area is based on an annual mean of average monthly solar insolation of 5.77 kWh per m^2 per day, which can be used to approximate the equivalent hours of full sun the location receives.[22] The maximum amount of 8.39 kWh per m^2 per day occurs in June while the minimum amount of 2.94 kWh per m^2 per day occurs in December, and such fluctuations in production are accounted for by sizing H_2 collection and treatment for the maximum monthly production rate at beginning-of-life.

The device and model design of the hydrogen production facility

The facility employs Z-scheme stacked reactor beds in modular raceway configurations, analogous to those used in algae-sourced biofuel production[23], as depicted in **Figure 2**. The raceway design is a shallow water pool with floating reactor cylinders for H_2 collection. Perforations in the transparent polymer film allow the O_2 generated in the lower reactor pool to vent to the atmosphere while limiting water loss due to evaporation. Piping systems allow water to flow into the main bed as well as into the HER reactor cylinders. Freely dispersed nanoparticles are suspended in the water within each respective HER and OER chamber to catalyze and enable the two-part water splitting reaction. The concentrations of nanoparticles in each chamber are set to fully capture the incident sunlight and appropriately apportion the split between reactions. The reactor cylinders are assumed to be slightly above atmospheric pressure (<1.3 bar), mitigating pressure-induced crossover of H_2 into the O_2 compartment and the subsequent formation of explosive mixtures of gases.[24] The H_2 gas leaving the reactor effluent separator is pressurized in a compression train to ~30 bar before entering the H_2 purification system (details on the balance of plant can be found in the **ESI**). While solar irradiance provides the energy needed to produce hydrogen, electricity is needed to operate controls and compress H_2 to 30 bar for pipeline injection. Hydrogen storage and distribution methods vary based on end uses and are thus considered outside the scope of this study. We assume electricity is provided by the grid for ancillary equipment, and water is delivered by a local utility before onsite deionization. For this study, we assume the electricity price is 2020 $0.03/kWh, which corresponds to average wholesale electricity prices currently possible in U.S. markets with plentiful wind.[25] The water price is assumed to be 2020 $0.00237/gal based on estimates for utility-scale water.

We model a modular raceway as being 20 m by 200 m (4,000 m^2). Assuming a 10% STH, 17 raceways are needed for a 1 metric tonnes per day (MTD) plant, and 819 raceways are needed for a 50 MTD plant. A sample plant layout for a 1 MTD plant is shown in **Figure 2**. To achieve low cost for large raceway designs like this, a geomembrane is laid directly down onto an excavated area to form the pool volume. The selected geomembrane is based on commercially available products for environmental remediation and lining applications, and consists of outer layers of linear-low density polyethylene and an inner core of resins. While no active circulation is assumed in the current design, a partition can be left in the middle of the raceway to form a circulation path if there is a need for water movement. Unlike algal-based biomass production, photocatalytic systems with stabilized suspensions may not require constant circulation to maintain performance. We expect that solar heating and evaporation induced temperature gradients have the potential to generate reasonable circulation currents in shallow ponds (<2 cm) to prevent suspended nanoparticles from settling onto the bottom of the pool. We assume the geomembrane lasts the lifetime of the plant (40 years).

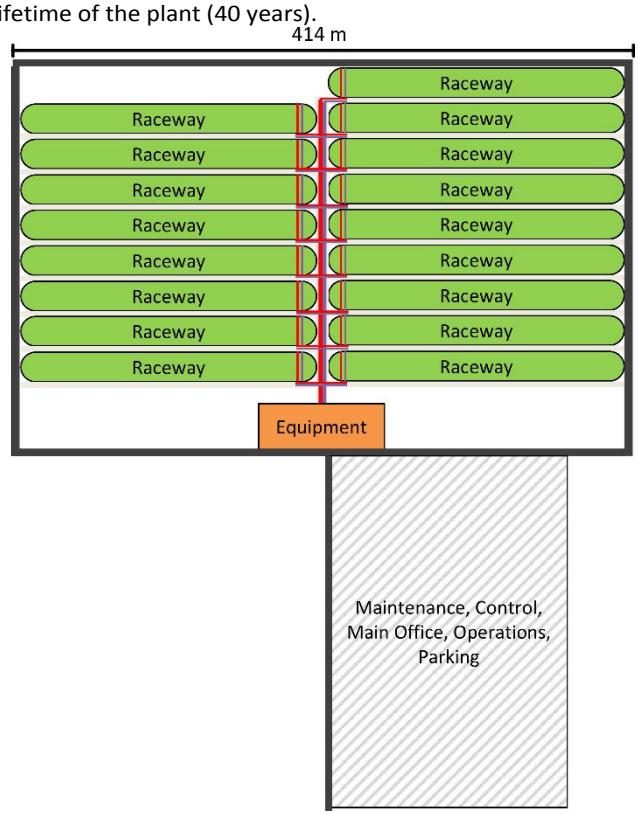

Figure 2. Facility layout for 1 MTD photocatalytic Type 2 Z-Scheme raceway system. 217 raceways are needed for 1 MTD plant assuming a solar-to-hydrogen conversion efficiency of 10%.

Reactor nanoparticles

For the purposes of cost modelling, we assume identical composite nanoparticles for the HER and OER photoabsorbers. As placeholder materials, the composite nanoparticles consist of a 40 nm Fe_2O_3 core with a 5 nm TiO_2 coating. Fe_2O_3 is a strong visible light absorber, making it a good representative oxide material in lieu of BiVO4 for the purposes of cost estimation.[26] We also include 1 wt% Pt as a "cocatalyst" that decorates the surface of the photocatalyst (see **Figure 1**). Pt was chosen as a representative precious metal constituent as iridium and platinum have shown to be effective water-splitting electrocatalysts in liquid alkaline and PEM electrolysis. The solar to hydrogen (STH) efficiency was assumed to be 10% based on total insolation to the surface of the raceway. This compares well with the STH technical target proposed by the Department of Energy (DOE) for dual bed photocatalyst hydrogen production for 2020 (5%) and Ultimate (10%).[27] We expect particle lifetime to be between 0.5-5 years to ensure the system never drops below 80% beginning-of-life catalytic performance. The base case design assumes a 1-year particle lifetime before replacement is needed, with cost modelling suggesting this leads to an attractive levelized cost of hydrogen. Note that under real operation, the STH performance of the nanoparticles is expected to degrade over time. Therefore, the specified STH efficiency should be considered the average performance over the lifetime of the particle. The equipment and piping is sized for this average operating condition.

The cost of the nanoparticles was estimated from the raw materials costs (including metal oxide precursor, dopant precursor, cocatalyst precursor, and solvent) and the synthesis cost (reaction, washing and filtering, doping, and photodeposition). Additional details can be found in the **ESI**. Depending on the annual production rate and the cost of the cocatalysts, we estimate that the nanoparticles will cost between \$100/kg to \$1,200/kg, without a manufacturer markup. For this study, we assume an additional 50% manufacturer markup, bringing the cost range to \$150/kg to \$1,800/kg. The base case particle cost is assumed to be \$450/kg, including a manufacturer markup, and based on a high manufacturing volume. This is lower than the DOE target for 2020 of \$500/kg, but higher than the ultimate target of \$300/kg. Calculations for light extinction suggest that 200 nm equivalent thickness of 40 nm particles is sufficient to capture all of the light entering the bed. The required nanoparticle loading for complete light usage is estimated to be 0.00105 kg/m^2.

Reactor cylinders

The floating hydrogen reactor cylinders contain particles that carry out the HER and collect the produced H_2. The hydrogen is assumed to fill the available headroom and passively leave the reactor cylinders as pressure increases. The top of the reactor cylinders is modelled as transparent high-density polyethylene (HDPE) at a thickness that allows 90% incident light transmission. The current model assumes an HDPE thickness of 0.25 in, which is commercially available product. The bottom of the reactor cylinders is modelled as a transparent electrospun polycarbonate filter membrane as it must allow the transmission of light and liquids between chambers but prevent the transfer of nanoparticles. Electrospun optically transparent fibrous membrane are expected to be possible using appropriate materials and fabrication method described by Xiao et al.[28] However, membranes currently available at commercial volumes are more focused on water filtration and medical applications and do not possess the optical transparency required for this application. Additional research and development will be needed to valid that a hydrophilic, transparent, high-durability materials can be manufactured at scale for this application. For this study, the authors developed a Design for Manufacture and Assembly® (DFMA®)[29] cost analysis for high-volume electrospun polycarbonate filter membrane and estimate the cost to be \$2.52/m^2 (2020 US\$).

Table 1. Key material and energy inputs and assumptions for a single raceway component for the two facility concepts of 1 metric tonne per day (MTD) and 50 MTD scales.

Parameter	Unit	1 MTD	50 MTD
Number of Raceways for system	#	17	819
Raceway Materials			
High-density polyethylene (HDPE) (top transparent film)	kg / raceway	33,400	33,400
Polycarbonate filter membrane (bottom ion bridge)	kg / raceway	53.7	53.7
Geomembrane	kg / raceway	3460	3460
Catalyst Nanoparticles			
Fe_2O_3 nanoparticles (as Fe)	kg / raceway	2.04	2.04
TiO_2 nanoparticles	kg / raceway	1.95	1.95
Platinum	kg / raceway	0.04	0.04
Piping System			
Polyvinylchloride (PVC) piping	kg / raceway	40	186
Stainless steel	kg / raceway	1004	305
Site Preparation and Construction			
Concrete	m^3 / raceway	14	3.0
Asphalt pavement	kg / raceway	94,400	29,800
Reinforcing steel	kg / raceway	666	141
Truck Transportation (total)	km	300	300
Operation			
Electricity input	kWh/kg H2	3.6	2.5
Water	L/kg H2	9.2	9.2
Maintenance			
Raceway cylinder replacement	yr	5	5
Nanoparticle replacement	yr	1	1

Sufficient sunlight is assumed to pass through the hydrogen reactor cylinders to enable the oxygen evolution reaction in the

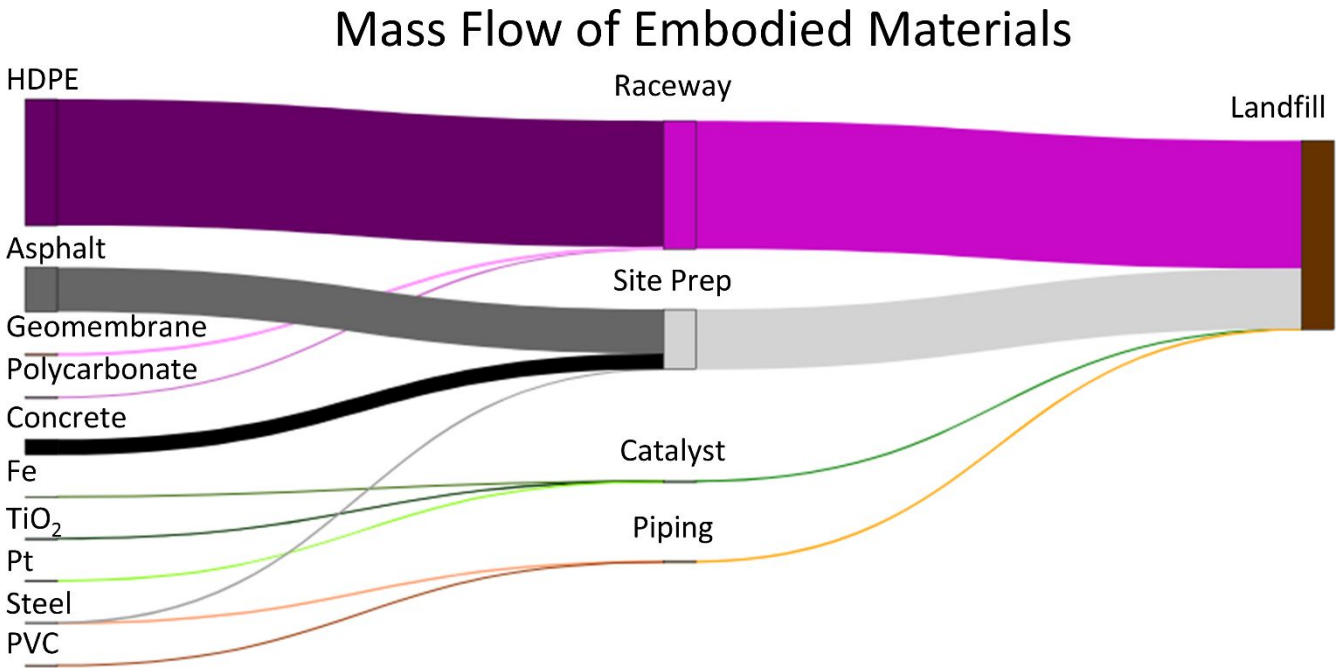

Figure 3. Flow of total mass (kg) of assessed input materials embodied in a 1 MTD facility from primary input to midpoint use to end-of-life. Electricity and water are neglected in the diagram as they are consumed in operation and do not fit material flow. HDPE: High density polyethylene. PVC: polyvinyl chloride.

oxygen reactor pool. The geometry of the reactor should be tuned such that half of the solar energy collected by the reactor is delivered to the hydrogen evolution reaction while the other half is delivered to the oxygen evolution reaction. Pilot studies are needed to optimize the size of the reactor cylinders, thickness of the HDPE in the cylinder walls, the depth of the pool, the perforated film length between cylinders, and the area of ion bridge needed to achieve steady state hydrogen production and safely manage seasonal fluctuations. In addition, the lifetime of the reactor cylinders needs to be experimentally validated. For this study, we assume the lifetime of raceway cylinders is 5 years which is consistent with heuristics for UV stabilized HDPE.[30] Future studies should consider whether oxygen and hydrogen crossover is sufficiently mitigated in the current design or if further mitigation is needed to ensure safe hydrogen production.

Analysis approach

The process model including balance of plant was developed and simulated in Aspen HYSYS® software (**Figure S2**). The total installed capital cost for a photocatalytic Type 2 Z-Scheme plant was estimated from bottom-up cost models that account for purchased equipment, installation costs, site preparation, and general overhead costs. Assumptions from the Hydrogen Analysis (H2A) production model, a peer-reviewed national laboratory-developed discounted cash flow model, were used to calculate the levelized cost of hydrogen (LCOH) production in 2020 $/kg-H2, which accounts for capital and operating costs.[31]

A hybrid life-cycle approach was used to develop an inventory of environmental impacts from all material and energy flows associated with the facility life cycle (**Figure S6**). These flows are converted to emissions based on specific emission factors (**Table S7**), or by using physical units-based input–output LCA models associated with the broader economic impacts of fuel and materials production, use, and end-of-life. Amount of material and energy consumption per raceway are shown in **Table 1** while **Figure 3** shows the flow of embodied materials from input to end-of-life. Full details of the life-cycle method are provided in the **ESI Notes 1-5**.

Results & discussion

Bottom-up total installed capital cost

The raceway consists of a reactor pool, floating reactor cylinders and support hardware (component costs are summarized in **Table S2**). The biggest capital costs are the geomembrane, which defines the pool volume and the polycarbonate filter membrane which forms the permeable barrier between the HER compartment and the OER compartment. The uninstalled reactor cost per solar incidence area is $7.14/m^2. This compares favourably with previously proposed cost targets by the Department of Energy (DOE) for photocatalytic panel electrodes where the Ultimate target was $100/m^2.[32] Note that less than 10% of the cost of this hypothetical photocatalytic panel electrode accounts for the light absorbers; the rest is associated with costs for encapsulation and manufacturing of the reactor.[33] All direct and installed capital costs associated with the raceways and balance of plant are included in **Table S2-S4** while greenfield construction related costs are included in **Table S5.** Like any greenfield project, siting can greatly affect construction costs, and we note the importance of site selection that may impact the cost of rural land (baseline value is $50,000/acre) and the need for surface levelling and road development. The configuration of raceways will impact costs mainly through changes to the balance of plant equipment, in

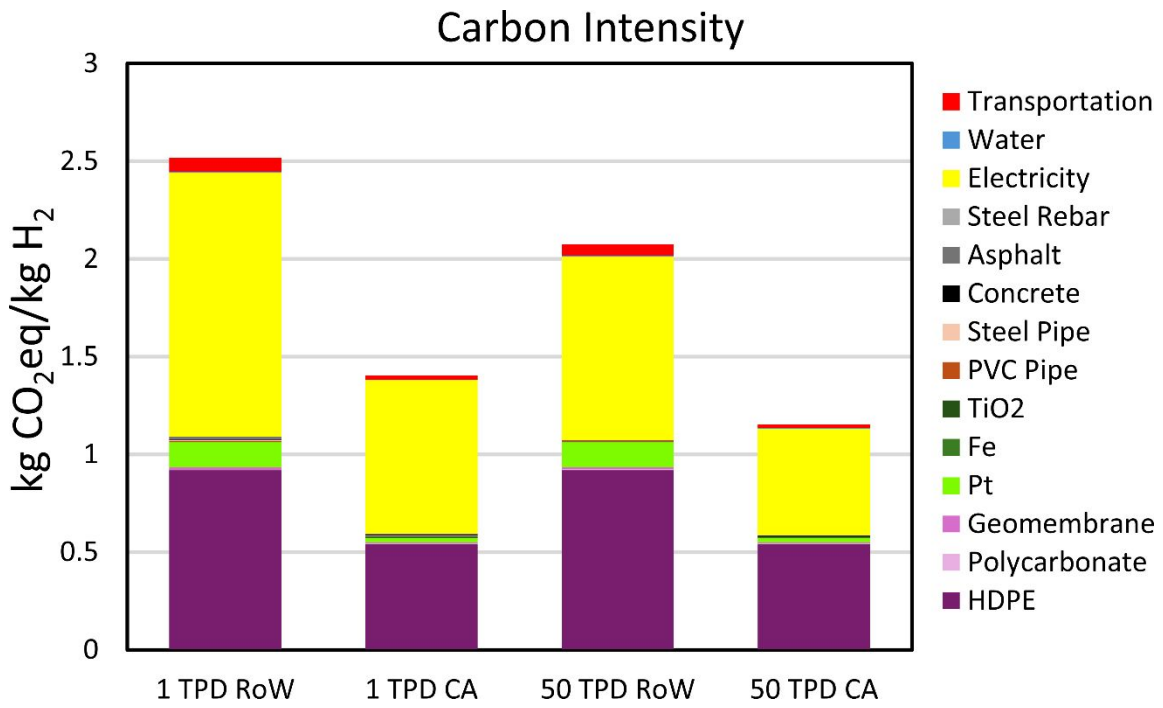

Figure 4: Comparison of carbon intensity for 1 MTD and 50 MTD facilities using either emissions factors representing 1) California (CA) operations or 2) rest of world (RoW) according to EcoInvent data. Water deionization EF is the same in all scenarios.

particular the need for piping and valves, which cost more than the raceways themselves.

Life Cycle Impacts

Similar to the levelized cost of hydrogen, the carbon intensity also decreases with facility size, going from 1.41 kg CO_2eq/kg H_2 for the 1 tonne per day facility to 1.15 kg CO_2eq/kg H_2. As a result, the photocatalysis technology used under the conditions described above shows great potential to meet clean hydrogen targets for a CI of <2-4 kg CO_2eq/kg H_2 produced.[34] The 18% decrease in emissions between scales can be attributed to economies of scale. Specifically BOP electricity use is more efficient at large scales, as is site preparation and construction. The raceways and internal components scale linearly with plant size and an improvement in carbon intensity is not observed for the larger plant design. Emissions are dominated by indirect emissions including electricity generation and plastics manufacturing. This suggests the carbon intensity of the system can be estimated with relative confidence once a facility design and location are established, unlike the levelized cost which may be more susceptible to changes in particle selection and manufacturing.

Despite electricity only being consumed to power the balance of plant, the source of electricity has a significant impact on emissions as BOP electricity is the leading contributor to emissions at 56%. Changing the emissions profile of electricity from the average California electricity grid mix to that derived from 100% solar photovoltaics results in a 45% decrease in emissions to 0.78 kg CO_2eq/kg H_2

Raceway materials (HDPE, polycarbonate membrane, and geomembrane) result in the second largest share of emissions, totalling 0.55 kg CO_2eq/kg H_2, with HDPE contributing the majority. This is proportional to the total amount of material consumed as seen in **Figure 3**, and highlights how different the system is compared with alkaline and PEM systems that require significant quantities of steel. Improving STH efficiency would have a clear beneficial impact on emissions, particularly through the reduced consumption of plastics (**Figure S8**). Raceway enclosure materials are subject to damage and wear, but the lifespan of such structures is poorly understood. Improving their durability could lower greenhouse gas emissions by minimizing replacements and plastic waste from photocatalytic hydrogen facilities, by 0.17 kg CO_2eq/kg H_2 (**Figure S8**). An additional uncertainty with the raceway materials lies in the production and end-of-life processes. Manufacturing in regions with emissive electricity grids can increase CI by as much as 0.56 kg CO_2eq, while using energy intensive extrusion manufacturing processes for plastics can increases emissions by 0.20 kg CO_2eq. As for end-of-life treatment, it is conservatively assumed that all plastics go to landfill and have no recovery of embodied emissions. However, conventional HDPE is readily recyclable, therefore, it may be reasonable to design operations such that HDPE sheeting from the raceway both may be recycled and made from recycled material in order to reduce material emissions (**Figure S8**).[35]

Ecoinvent is a commonly used database for gathering emission factors for LCA, and we run our LCA model to explore the impact of using global supply chains and emission factors, rather than emission factors that represent local California and United States supply chains and energy systems. **Figure 4** shows the resulting CI for both 1 and 50 MTD scenarios with two sets of emission factors. The base case results discussed so far use emission factors sourced from literature to be specific to California where possible, and for the US where it is not.

Material manufacturing and electricity generation in particular are very location specific. The Ecoinvent database was used to source "rest of the world" EFs which represent weighted averages based on global data and assumptions and are higher across all inputs except concrete and polycarbonate production. The catalyst materials, specifically platinum, are subject to major changes in their emission contribution due to differences in EF, and this can be due to assumptions around the material sourcing as well as refining and production processes used. Given the minor amounts of platinum used overall (**Table 1**), emission contributions can far outweigh the relative amount of material consumed so choosing the most representative EF for the project conditions is imperative. Transportation of materials to the hydrogen facility and to landfills, and catalyst manufacturing are minor contributors to the CI. Transportation emissions are highly variable and may be higher if greater distances are assumed but may also be lower with the adoption of zero or near-zero emission vehicles and as fuel efficiency continues to improve.

The promising performance of this PC hydrogen production facility with respect to carbon intensity prompts a corresponding assessment of the energy return on energy invested (EROEI). Such an assessment evaluates the embodied and operational inputs to the system relative to the energy output from hydrogen. This study uses methods derived for energy payback time and EROEI of solar PV systems.[36,37] The high carbon intensity of input materials, in particular plastics and platinum, corresponds to energy associated with procurement and processing. This is evident as the system yields an EROEI of 2.47 with a payback time of 16.2 years of operation. While this EROEI is suboptimal for energy systems as it is below 3 as suggested by Hall et al. (2009), it does pass the viability threshold of 1, demonstrating a net return on energy invested.[38] The leading sources of energy consumption that give this system a suboptimal EROEI are platinum, HDPE, and grid electricity.

As the Ecoinvent database allows for rapid analysis of other critical impact categories, we include these results for global scenarios. Emissions in freshwater ecotoxicity showed the greatest levelized impact with 110 cumulative toxicity units (CTU) per kg H_2. While this is a notable concern, it is primarily due to electricity generation from fossil fuels, followed by the sourcing of platinum and manufacturing of asphalt. These emissions come from the combined upstream and operational use of the materials, consistent with the parameters used for CI. However, since Pt and electricity are used heavily in PEM electrolysis systems, the use of Pt in PC systems is not a comparative disadvantage. Other impact areas assessed include ozone depletion potential, human toxicity (both carcinogenic and non-carcinogenic), acidification potential, photochemical oxidation potential, and eutrophication potential. These other areas have minor impacts in comparison to those discussed above and are more fully discussed in **Note S5.**

While estimating the direct consumption of water for hydrogen production is straightforward, consideration of treatment processes and evaporation is not. However, the use of perforated reactor cylinders limits evaporation and, within this study, the impact of evaporation impact is considered negligible. Given the use of water as the key feedstock in electrolysis, future research should explore the capacity to use rainwater to supply feedstock water, especially if robust treatment of the water is not needed to maintain high STH efficiency. Rainwater is not considered in this study as it does not constitute a reliable source of water, especially in the US southwestern desert-location sited for this study, but it also cannot be avoided in cases such as the one presented here where raceways are not fully sheltered. Finally, with the increasing emphasis on a hydrogen economy, further analysis of potential hydrogen leakage emissions will become important as there is growing evidence that hydrogen emissions lead to increased CH_4 global warming intensity via atmospheric reactions.[39]

Levelized cost of hydrogen

LCOH was calculated using the aforementioned H2A model for 1 MTD and 50 MTD hydrogen plants. The performance and capital cost input assumptions for these hypothetical systems and the associated H2A results are shown in **Table S2-S6**. Note that these results are contingent on material sets, photoabsorber durability, and photoabsorber performance that have not yet been demonstrated. The levelized cost of hydrogen for the 1 MTD and 50 MTD cases with a 10% solar-to-hydrogen efficiency are summarized in **Figure 5** broken down into capital costs, fixed operations and maintenance (primarily labor and maintenance costs), and utilities (primarily electricity costs). Levelized cost of hydrogen decreases by 75% through economies of scale evaluated, suggesting a very competitive production price of $1.89/kg for a 50 MTD plant. The 1 MTD plant suffers from high operation and maintenance costs consistent with a low production rate plant. The electricity price is assumed to be $0.03/kWh with 100% availability which represents an aspirational target for low cost, wholesale grid

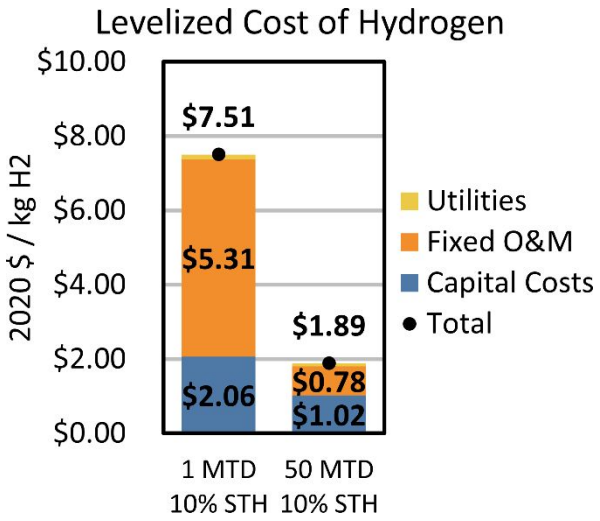

Figure 5. Projected levelized cost of hydrogen (LCOH) summarized by sub-component for a photocatalytic Type 2 Z-Scheme plant with capacity of 1 MTD and 50 MTD and a 10% solar-to-hydrogen efficiency assuming a baseline capacity factor of 97% and electricity price of $0.03/kWh.

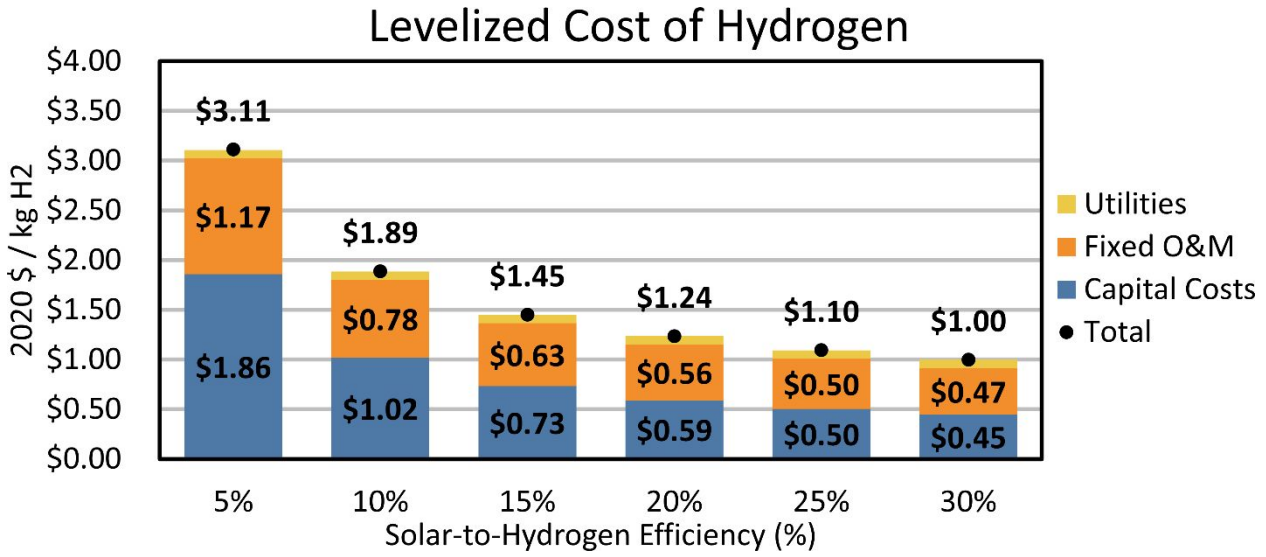

Figure 6. Projected levelized cost of hydrogen (LCOH) summarized by sub-component for a photocatalytic Type 2 Z-Scheme plant with capacity of 50 MTD and the solar-to-hydrogen efficiency varied from 5% to 30% assuming a baseline capacity factor of 97% and electricity price of $0.03/kWh.

electricity prices. If conventional grid-based electricity prices were used, the cost of electricity would be almost two times greater depending on the region of the world. However, this would have only a marginal impact on the levelized cost of hydrogen as **Figure 5** shows that utility costs comprise <5% the total LCOH.

To understand the impact of solar-to-hydrogen efficiency on the levelized cost of hydrogen, the STH efficiency was parametrically varied between 5% and 30% for a fixed 50 MTD plant. Increasing STH efficiency reduces the number of raceways which reduces both the capital costs and the labor costs as shown in **Figure 6**. At 30% STH efficiency, the LCOH drops to $1/kg which would meet the Hydrogen Earthshot target as specified by the U.S. Department of Energy. Note that 30% STH represents an ambitious, ultimate research target for Type-2 architectures. Even at a more conservative 10% STH efficiency, our analysis indicates an LCOH competitive with today's natural gas-based hydrogen (~$1-2 /kg), showing that moderate STH gains alone could justify further development.

Significant uncertainty still remains in what the upper limit of the catalyst particle lifetime will be under real, diurnal solar conditions. In particular, the catalyst particles are subject to a long term aqueous environment and may encounter biological growth and poisoning from environmental materials. Current particle performance in the lab is mostly limited to 100's of hours with the exception of a recent demonstration at a scale of 100 m^2 demonstrating stability of photocatalytic particles over several days and on the order of 1000 h under simulated sunlight.[40] To assist in developing a research and development roadmap, a 2D sensitivity analysis for LCOH was conducted across solar-to-hydrogen efficiency and particle lifetime (**Figure 7**). We assume the floating reactor cylinders have a fixed lifetime of 5 years and that the cost of the particles and floating reactor cylinders are fixed. **Figure 7** suggests that the LCOH is largely insensitive to particle lifetime beyond a year. Nanoparticle costs are significant relative to the initial cost of

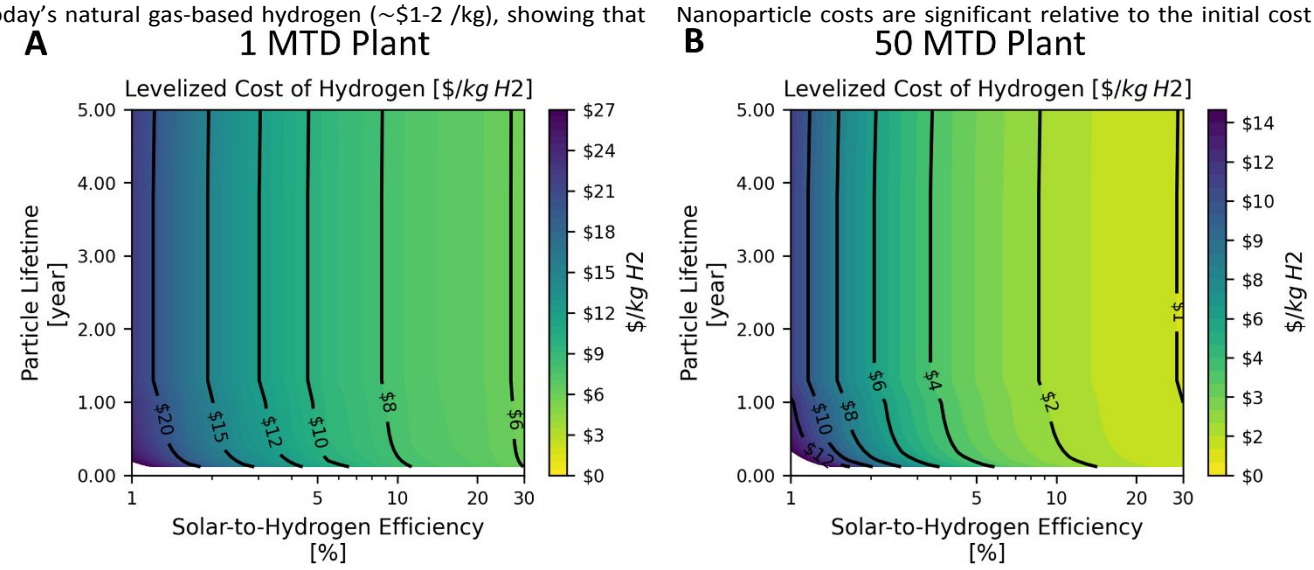

Figure 7. Projected levelized cost of hydrogen (LCOH) as a function of solar-to-hydrogen efficiency and particle lifetime for A) a 1 MTD plant and B) a 50 MTD plant.

the reactor. However, as nanoparticle lifetimes increase, the initial investment of the plant and the ongoing cost of maintaining and operating the large number of raceways tend to dominate the levelized cost of hydrogen. **Figure 7A** shows that there is a limit to the LCOH achievable for a small system regardless of the catalyst efficiency. **Figure 7B** suggests that the pathway to achieving a $1/kg LCOH is by increasing the particle lifetime to 1 year and driving the solar-to-hydrogen efficiency as high as possible (near 30% STH).

The current model assumes there is no water purification post-deionization and no significant evaporation losses. However, addition processing needs and water makeup could lead to significant changes in model design and costs due to the need for continuous water purification and greater flow of water inlet. Based on the low emissions associated with operation of the plant, the modelled plants may qualify for clean hydrogen incentives, such as the production tax credit from the U.S. Inflation Reduction Act. As such, assuming the maximum production tax credit of $3 per kg of hydrogen is applied (applicable to systems with <0.45 kg CO_{2eq} per kg H_2 production emissions), the levelized cost may be as low as $4.51/kg for the 1 MTD facility and essentially *free* with <$0/kg for the 50 MTD facility. If hydrogen is sold as a low-carbon fuel in California, the cost could be further reduced based on the type of fossil fuel avoided.

Conclusions

In this work we have presented a plausible pathway to achieving low cost, sustainable hydrogen using a photocatalytic Z-scheme electrochemical raceway system. In particular, using this raceway system enables a cost competitive reactor cost with low CI potentially below 1 kg CO_{2eq}/kg H_2. Future research and development of particle catalysts should focus on meeting a particle lifetime of >0.5 years and a solar-to-hydrogen efficiency of >10%.

There are remaining challenges that must be solved prior to commercial implementation of the raceway hydrogen production system:

(i) An acceptable pair of HER and OER photocatalytic particles must be developed with sufficiently long durability and solar-to-hydrogen efficiency in solution.
(ii) Development and selection of an acceptable ion membrane will require research and development in collaboration with membrane manufacturers.
(iii) The particle slurry must be stable in suspension, even under diurnal conditions, which may require additional balance-of-plant to manage.
(iv) The raceway geometry must be optimized to maximize performance and achieve acceptable safety including water depth, reactor cylinder sizing, and particle density.
(v) Using floating reactor cylinders to collect H_2 and the ability of passive diffusive species transport to maintain redox shuttle concentrations at an acceptable level needs further analyses and experimental work
(vi) Many redox shuttles used in Z-scheme systems have challenges that stem from competitive light absorption, pH-specific stability and speciation, and solubility limits, which need to be more carefully assessed and incorporated in the design and LCOH estimates.
(vii) Performance must be tested under expected water conditions which may include particulate matter introduced from rainwater and possible organic material. Algae suppressants may be needed to prevent organic growth.
(viii) Stability of reactor cylinder materials including the HDPE top layer and the ion membrane bottom layer must be tested under diurnal and seasonal conditions.
(ix) Reduction of plastics and platinum consumption are necessary for life cycle and EROEI improvements.

The authors encourage the development of pilot raceway hydrogen production systems to begin testing the potential of this approach to green hydrogen production.

Author Contributions

S. Collins conducted the investigation of the life-cycle analysis, evaluation of carbon intensity, and energy return on energy invested. Y. Acevedo conducted the investigation of the technoeconomic analysis of the plant. D. V. Esposito, R. Bala Chandran, and S. Ardo participated in conceptualization and supervision of project activities. B. D. James and H. Breunig participated in project administration and supervision. All the authors contributed to writing and proofing the manuscript.

Conflicts of interest

There are no conflicts to declare.

Data Availability Statement

The data supporting this article have been included as part of the Supplementary Information.

Acknowledgements

The authors gratefully acknowledge support from the U.S. Department of Energy under Contract No. DE-EE0009629 with Strategic Analysis, Inc. and under Contract No. DE-AC02-05CH11231 with the Lawrence Berkeley National Laboratory. The authors would also like to thank Raven Engineered Films, Sartorius, Sterlitech, and GVS for their advice on prospective materials for the geomembrane and the ion bridge.

Notes and references

1 B. S. Pivovar, M. F. Ruth, D. J. Myers and H. N. Dinh, *Electrochem. Soc. Interface*, 2021, **30**, 61–66.
2 K. Ayers, N. Danilovic, R. Ouimet, M. Carmo, B. Pivovar and M. Bornstein, *Annual Review of Chemical and Biomolecular Engineering*, 2019, **10**, 219–239.
3 M. J. Ginsberg, D. V. Esposito and V. M. Fthenakis, *Cell Reports Physical Science*, 2023, **4**, 101625.

4 M. Hubert, D. Peterson, E. Miller, J. Vickers, R. Mow and C. Howe, *Clean Hydrogen Production Cost Scenarios with PEM Electrolyzer Technology*, Department of Energy, 2024.
5 A. Kusoglu, *Electrochem. Soc. Interface*, 2022, **31**, 47–52.
6 B. A. Pinaud, J. D. Benck, L. C. Seitz, A. J. Forman, Z. Chen, T. G. Deutsch, B. D. James, K. N. Baum, G. N. Baum, S. Ardo, H. Wang, E. Miller and T. F. Jaramillo, *Energy & Environmental Science*, 2013, **6**, 1983–2002.
7 H. Nishiyama, T. Yamada, M. Nakabayashi, Y. Maehara, M. Yamaguchi, Y. Kuromiya, Y. Nagatsuma, H. Tokudome, S. Akiyama, T. Watanabe, R. Narushima, S. Okunaka, N. Shibata, T. Takata, T. Hisatomi and K. Domen, *Nature*, 2021, **598**, 304–307.
8 B. Moss, O. Babacan, A. Kafizas and A. Hankin, *Advanced Energy Materials*, 2021, **11**, 2003286.
9 D. M. Fabian, S. Hu, N. Singh, F. A. Houle, T. Hisatomi, K. Domen, F. E. Osterloh and S. Ardo, *Energy Environ. Sci.*, 2015, **8**, 2825–2850.
10 H. Dotan, N. Mathews, T. Hisatomi, M. Grätzel and A. Rothschild, *Journal of Physical Chemistry Letters*, 2014, **5**, 3330–3334.
11 J. Kibsgaard and I. Chorkendorff, *Nat Energy*, 2019, **4**, 430–433.
12 M. R. Shaner, H. A. Atwater, N. S. Lewis and E. W. McFarland, *Energy Environ. Sci.*, 2016, **9**, 2354–2371.
13 J. W. Ager, M. R. Shaner, K. A. Walczak, I. D. Sharp and S. Ardo, *Energy & Environmental Science*, 2015, **8**, 2811–2824.
14 M. T. Spitler, M. A. Modestino, T. G. Deutsch, C. X. Xiang, J. R. Durrant, D. V. Esposito, S. Haussener, S. Maldonado, I. D. Sharp, B. A. Parkinson, D. S. Ginley, F. A. Houle, T. Hannappel, N. R. Neale, D. G. Nocera and P. C. McIntyre, *Sustainable Energy Fuels*, 2020, **4**, 985–995.
15 G. Zhao, M. R. Kraglund, H. L. Frandsen, A. C. Wulff, S. H. Jensen, M. Chen and C. R. Graves, *International Journal of Hydrogen Energy*, 2020, **45**, 23765–23781.
16 E. Cetinkaya, I. Dincer and G. F. Naterer, *International Journal of Hydrogen Energy*, 2012, **37**, 2071–2080.
17 K. Bareiß, C. de la Rua, M. Möckl and T. Hamacher, *Applied Energy*, 2019, **237**, 862–872.
18 R. Sathre, C. D. Scown, W. R. Morrow, J. C. Stevens, I. D. Sharp, J. W. Ager, K. Walczak, F. A. Houle and J. B. Greenblatt, *Energy and Environmental Science*, 2014, **7**, 3264–3278.
19 Q. Jia, A. Iwase and A. Kudo, *Chem. Sci.*, 2014, **5**, 1513.
20 D. K. Lee and K.-S. Choi, *Nat Energy*, 2017, **3**, 53–60.
21 Y. Kuang, Q. Jia, G. Ma, T. Hisatomi, T. Minegishi, H. Nishiyama, M. Nakabayashi, N. Shibata, T. Yamada, A. Kudo and K. Domen, *Nat Energy*, 2016, **2**, 16191.
22 M. Sengupta, Y. Xie, A. Lopez, A. Habte, G. Maclaurin and J. Shelby, *Renewable and Sustainable Energy Reviews*, 2018, **89**, 51–60.
23 R. Davis, J. Markham, C. Kinchin, N. Grundl, E. C. D. Tan and D. Humbird, *Process Design and Economics for the Production of Algal Biomass: Algal Biomass Production in Open Pond Systems and Processing Through Dewatering for Downstream Conversion*, 2016.
24 S. Haussener, C. Xiang, J. M. Spurgeon, S. Ardo, N. S. Lewis and A. Z. Weber, *Energy Environ. Sci.*, 2012, **5**, 9922.
25 J. Seel, D. Millstein, A. Mills, M. Bolinger and R. Wiser, *Advances in Applied Energy*, 2021, **4**, 100073.
26 Q. Mei, F. Zhang, N. Wang, Y. Yang, R. Wu and W. Wang, *RSC Adv.*, 2019, **9**, 22764–22771.
27 DOE Technical Targets for Hydrogen Production from Photoelectrochemical Water Splitting, https://www.energy.gov/eere/fuelcells/doe-technical-targets-hydrogen-production-photoelectrochemical-water-splitting, (accessed 14 June 2024).
28 Y. Xiao, H. Luo, R. Tang and J. Hou, *Polymers*, 2021, **13**, 506.
29 G. Boothroyd, P. Dewhurst and W. A. Knight, *Product Design for Manufacture and Assembly, Third Edition*, CRC Press, 2010.
30 The Plastic Sheeting Gurus!, Which Plastic Sheeting Lasts the Longest Under What Conditions?, https://www.globalplasticsheeting.com/our-blog-resource-library/which-plastic-sheeting-lasts-the-longest-under-what-conditions.
31 H2A, https://www.nrel.gov/hydrogen/h2a-production-models.html, (accessed 1 March 2021).
32 *DOE Technical Targets for Hydrogen Production from Photoelectrochemical Water Splitting*, U.S. D.O.E. Hydrogen and Fuel Cell Technologies Office.
33 B. D. James, G. N. Baum, J. Perez and K. N. Baum, *Technoeconomic Analysis of Photoelectrochemical (PEC) Hydrogen Production*, 2009.
34 Clean Hydrogen Production Standard Guidance | Hydrogen Program, https://www.hydrogen.energy.gov/library/policies-acts/clean-hydrogen-production-standard, (accessed 14 June 2024).
35 *Life Cycle Impacts for Postconsumerrecycled Resins: PET, HDPE, and PP*, The Association of Plastic Recyclers, 2018.
36 R. Bhandari, C. A. Trudewind and P. Zapp, *Journal of Cleaner Production*, 2014, **85**, 151–163.
37 K. P. Bhandari, J. M. Collier, R. J. Ellingson and D. S. Apul, *Renewable and Sustainable Energy Reviews*, 2015, **47**, 133–141.
38 C. A. S. Hall, S. Balogh and D. J. R. Murphy, *Energies*, 2009, **2**, 25–47.
39 M. B. Bertagni, S. W. Pacala, F. Paulot and A. Porporato, *Nat Commun*, 2022, **13**, 7706.
40 H. Nishiyama, T. Yamada, M. Nakabayashi, Y. Maehara, M. Yamaguchi, Y. Kuromiya, Y. Nagatsuma, H. Tokudome, S. Akiyama, T. Watanabe, R. Narushima, S. Okunaka, N. Shibata, T. Takata, T. Hisatomi and K. Domen, *Nature*, 2021, **598**, 304–307.

Data Availability Statement:

Levelized cost and carbon intensity of solar hydrogen production from water electrolysis using a scalable and intrinsically safe photocatalytic Z-scheme electrochemical raceway system

Stephanie Collins*[a], Yaset Acevedo*[b], Daniel V. Esposito[c], Rohini Bala Chandran[d], Shane Ardo[e], Brian D. James*†[b], Hanna Breunig*†[a]

a. Energy Analysis and Environmental Impacts Division, Energy Technology Area, Lawrence Berkeley National Laboratory, Berkeley, California, U.S.A., 94720
b. Strategic Analysis Inc., Arlington, Virginia, U.S.A., 22203
c. Columbia University, New York, New York, U.S.A., 10027
d. University of Michigan, Ann Arbor, Michigan, U.S.A., 48109
e. University of California, Irvine, Irvine, California, U.S.A., 92697
* These authors contributed equally to this work.
† Co-corresponding authors

The data supporting this article have been included as part of the Supplementary Information.